

SURFACE INSTABILITY OF THE PLANE LAYER OF CONDUCTING LIQUID

I. Kolesnichenko, S. Khripchenko

Institute of Continuous Media Mechanics, Perm, Russia

In this paper, the behavior of the plane layer of conducting liquid with a free surface is studied. The layer is assumed to be subjected to volumetric electromagnetic forces caused by the interaction between the electrical current, flowing through the layer, and the magnetic field. The vector of these forces lies in the layer plane. Because of the applied forces, the layer surface can be fixed at equilibrium position. It is found that under certain parameters this position can be unstable against disturbances. The probability of the vortex flow in the layer could decrease the stability threshold of the equilibrium position of the layer surface against disturbances.

1. Introduction. Processes taking place in a liquid metal layer with a free surface, the thickness of which is less than its length and width, are broadly studied. Under electromagnetic forces generated in the layer, the free surface can be fixed at equilibrium position. It can hold at this position regardless of whether the vortex flow is absent or present. In the first case, electromagnetic forces are only potential and, in the second, they involve a vortex component. Under certain parameters, the equilibrium position of the surface is unstable against small disturbances. Hence, a regime of surface non-decaying oscillations can be reached. This phenomenon has been observed in some technological processes developed for operating with liquid metal layers with a free surface such as aluminum electrolysis, stirring of flows generated in flat metal layers, and melting of flat metal layers. In these processes, the electrical current, passing through the liquid metal along or across the layer, is used. Non-decaying and, especially, increasing surface oscillations are undesirable but probable in the mentioned processes.

Electromagnetic forces generated in a layer due to the interaction between the electrical current and its own magnetic field (or an external field, if present) can be potential originally. As a rule, this implies the availability of the equilibrium position, at which the liquid flow is absent, and the free surface gets some shape defined by the balance between electromagnetic and gravity forces. The disturbance of the equilibrium surface position perturbs the electrical current field. The instability phenomenon is possible when the vector of electromagnetic forces has a vertical component (the buoying forces) [1], and when the vector of electromagnetic forces lies in the layer plane [2, 3]. The disturbance of the electrical current caused by the layer thickness nonuniformity along the current vector direction produces the vortex component of electromagnetic forces. This is the condition for generating the electrovortex flow (EVF) [4].

Another condition for EVF generation is the nonuniformity of own magnetic field (or the external field) along the current direction [4]. The electromagnetic forces are assumed to have the vortex component originally. One way of generating these vortex forces suggests that the layer should be placed into a gap between the ferromagnetic slabs. The value of the gap between the slabs must vary along the electrical current streamlines. This can be achieved by inclining one of the slabs in the current direction [4]. If the slab is inclined across the current direction, the volume electromagnetic forces are potential [5] and they fail to generate as

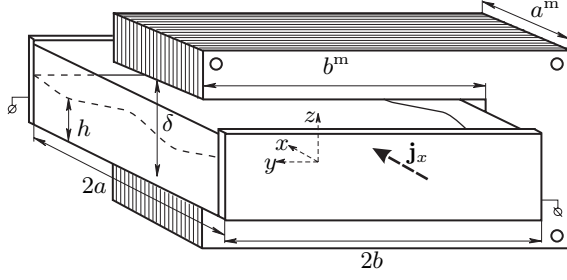


Fig. 1. Schematic representation of the examined plane layer.

initially vortex flow. However, such flow can appear owing to the isothermal MHD-instability [5, 6]. The value of the gap can be changed from a certain value up to infinity by restricting the slab size in the plane. If the electrical current passes normally to the layer, or an alternating magnetic field is generated perpendicular to the layer in some restricted areas of layer plane, then another way of EVF generation is possible. However, the contour of such areas has to be different from the circle. In these cases, the EVF with four, eight or more eddies is generated [7, 8, 9], and the surface may become unstable. The free surface oscillations were observed experimentally for some set of parameters in the case of EVF with four eddies [9]. Two effects initiated the surface instability: the nonlinear interaction between EVF and surface oscillations, and the change in electrical current density produced by the surface oscillations [8]. The second effect can be described for a two-layer liquid as follows. The oscillations of the interface between layers change the effective electrical conductivity of this two-layer system and vary the electrical current density and electromagnetic forces.

When the electrical current passes along the plane of the layer, the current density can be changed only due to the surface oscillations with the wave vector directed along the current density vector \mathbf{j} . The layer is placed either in the external magnetic field, or in the gap between ferromagnetic slabs, or in the gap of the ferromagnetic C-core. The magnetic field \mathbf{B} thus generated can penetrate the whole layer plane or only its part (Fig. 1). In the latter case, one can observe the EVF generation, which decreases the stability threshold of the equilibrium position of the layer surface against disturbances.

2. Equations of motion of the liquid. The plane liquid layer with a free surface differs from the layer with a solid cover by hydrostatic pressure. The pressure gradient is expressed in terms of the layer height $h(x, y, t)$ as $\nabla P = \rho g \nabla h$. It means that at generating of, for example, a vortex flow in this layer, an excessive pressure provokes the growth of the layer height, whereas the reduced pressure – decrease. This phenomenon can be observed in the center of the rotating layer of the liquid in the form of a funnel. The electromagnetic forces in the layer plane $\mathbf{F}(x, y, t) = (F_x, F_y, 0)$ generate the flow of a conducting fluid with a velocity $\mathbf{W}(x, y, z, t) = (W_x, W_y, W_z)$. The flow is described by the equation of magnetohydrodynamics, the equation of discontinuity and the boundary conditions for velocity and surface height:

$$\partial_t \mathbf{W} + (\mathbf{W} \nabla) \mathbf{W} = -G \nabla h + \Delta \mathbf{W} + S \beta \gamma \mathbf{F}^{\text{em}}, \quad (1)$$

$$\text{div} \mathbf{W} = 0, \quad (2)$$

$$\mathbf{W}(\pm a, \pm b, z, t) = 0, \quad \mathbf{W}(x, y, 0, t) = 0, \quad W_z(x, y, h, t) = \frac{dh}{dt}, \quad (3)$$

$$\frac{\partial h}{\partial x}(\pm a, y, t) = \frac{S \beta \gamma}{G} F_x^{\text{em}}(\pm a, y, t), \quad \frac{\partial h}{\partial y}(x, \pm b, t) = \frac{S \beta \gamma}{G} F_y^{\text{em}}(x, \pm b, t). \quad (4)$$

The main linear dimensions assumed are (Fig. 1) the layer half-length a , half-width b , horizontal thickness d , the length $a^m = |x_2 - x_1|$ and the width $b^m = |y_2 - y_1|$ of ferromagnetic slabs, the parameter δ , related to the magnetic field, and the value of overlap of the layer plane by the ferromagnetic slab $\xi = a^m b^m / 4ab$. For the layer placed in the gap between the ferromagnetic poles, δ is the gap value. In (1), we use the noninductive approximation, which holds valid for $\text{Rm} \ll \delta/2b$ [10]. Dimensionless parameters are written as

$$\mathbf{G} = \frac{gd^3}{\nu^2}, \quad \mathbf{S} = \frac{I_0^2 \mu_0}{4\rho\nu^2}, \quad \beta = \frac{d}{b}, \quad \gamma = \frac{d}{\delta}.$$

Since we consider the plane liquid layers (when $\beta \sim 0.1$), the shallow water approximation is used that holds valid for small gradients of changes in surface height ($\partial_x h, \partial_y h \sim 0.1$) [5, 11, 12]. In this case, the system of equations and boundary conditions (1)–(3) take the two-dimensional form:

$$\frac{\partial V_x}{\partial t} + \frac{\partial(V_x V_x q)}{\partial x} + \frac{\partial(V_x V_y q)}{\partial y} + V_x r \frac{dh}{dt} = -Gh \frac{dh}{dx} + \Delta V_x + \kappa V_x + \mathbf{S} \beta \gamma h F_x, \quad (5)$$

$$\frac{\partial V_y}{\partial t} + \frac{\partial(V_x V_y q)}{\partial x} + \frac{\partial(V_y V_y q)}{\partial y} + V_y r \frac{dh}{dt} = -Gh \frac{dh}{dy} + \Delta V_y + \kappa V_y + \mathbf{S} \beta \gamma h F_y, \quad (6)$$

$$\frac{\partial h}{\partial t} + (\mathbf{V} \nabla) h = -\nabla \cdot \mathbf{V}, \quad (7)$$

$$\mathbf{V}(\pm a, \pm b, t) = 0. \quad (8)$$

Boundary condition (4) for the layer height remains unchanged. To derive system of equations (5)–(8), the vector of three-dimensional velocity field was represented as the product $W_x = V_x f$, $W_y = V_y f$ of the two-dimensional vector with components, which are a local flow-rate $\mathbf{V}(x, y, t) = (V_x, V_y)$, and a normalized profile function:

$$f(z, \alpha, h) = \frac{-4\alpha(\text{sh}(\alpha z) - \text{sh}(2\alpha h) + \text{sh}(-\alpha z + 2\alpha h))\text{sh}(\alpha h)\text{ch}(\alpha h)}{\text{sh}(2\alpha h)(4\alpha h \text{sh}(\alpha h)\text{ch}(\alpha h) + e^{-2\alpha h}(2e^{2\alpha h} - e^{4\alpha h} - 1))}, \quad (9)$$

$$\alpha = \text{Ha} B, \quad \text{Ha} = \frac{I_0 \mu_0 \gamma}{2} \sqrt{\frac{\sigma}{\eta}}, \quad \int_0^h f(z, \alpha, h) dz = 1.$$

Then, we performed integration over the layer from 0 to h . This gives the following three functions in equations (5) and (6):

$$q(\alpha, h) = \int_0^h f^2(z, \alpha, h) dz = \alpha(-16\alpha h e^{4\alpha h} + 32\alpha h e^{4\alpha h} \text{ch}^4(\alpha h) - 16\alpha h e^{4\alpha h} \text{ch}^2(\alpha h) - 6e^{2\alpha h} + 6e^{6\alpha h} - 3e^{8\alpha h} + 3)/2(4\alpha h \text{sh}(\alpha h)\text{ch}(\alpha h)e^{2\alpha h} + 2e^{2\alpha h} - e^{4\alpha h} - 1)^2, \quad (10)$$

$$r(\alpha, h) = f(z = h, \alpha, h), \quad (11)$$

$$\kappa(\alpha, h) = \int_0^h \frac{\partial^2 f(z, \alpha, h)}{\partial z^2} dz = \frac{4\alpha^2(-2e^{2\alpha h} + 1 + e^{4\alpha h})}{4h\alpha \text{sh}(\alpha h)\text{ch}(\alpha h)e^{2\alpha h} + 2e^{2\alpha h} - e^{4\alpha h} - 1}, \quad (12)$$

the latter of which defines friction at the bottom. However, this function can be used when $\xi = 1$. In the case of $\xi < 1$, the vortex flow appears in the layer and the friction function κ is assumed equal to $(\kappa_1 + \kappa_2 |\mathbf{V}|)/2$, as in [3, 11, 12].

3. Electromagnetic forces. In the previous section, we have already said that the vector of electromagnetic forces lies in the layer plane. The electrical current I_0 passes between the vertical walls, $x = -a$ and $x = a$ (Fig. 1). The current density unit (defined for the horizontal position of the surface) is equal to $j_0 = I_0/(2db)$. For a non-horizontal surface of the layer, the current density $\mathbf{j} = (j_x, 0, 0)$ is defined in terms of the cross-sectional area (in a dimensionless form)

$$\Pi^i(x, t) = \frac{\beta}{2} \int_{-b}^b h(x, y', t) dy', \quad j_x(x, t) = 1/\Pi^i(x, t). \quad (13)$$

In this study, we consider the external magnetic field \mathbf{B}^e and the magnetic field of electrical current \mathbf{B}^i , which is amplified in the gap between the ferromagnetic slabs. The vertical field component with the dimension value $B_0 = I_0\mu_0/2\delta$ is much larger than the horizontal one. Therefore, we assume that $\mathbf{B} = (0, 0, B_z)$ [5]. The slabs may cover the area with the liquid metal in the plane only partly ($\xi < 1$). Let us write $\Omega^m = (x, y : x \in [x_1, x_2], y \in [y_1, y_2])$ for the overlap area, which may coincide with the layer area ($\xi = 1$). The magnetic field of the electrical current between the slabs will be determined using the Ampere law. Thus, we have

$$B_z^*(x, y, t) = j_x(x, t)\Pi^m(x, y, t) = j_x(x, t)\beta \int_y^{0^m} h(x, y', t) dy', \quad (x, y) \in \Omega^m. \quad (14)$$

The function of zero magnetic field $0^m(x, t)$ is the coordinate value $y \in [y_1, y_2]$ where $B_z^i(x, 0^m, t) = 0$, is defined by minimizing the functional $|\Pi^m(x, y_1, t) - \Pi^m(x, y_2, t)| \rightarrow 0$. For ferromagnetic cores (ferromagnetic slabs fitted with a one-sided jumper), 0^m is placed at the edge of the layer plane in the jumper area. For ferromagnetic slabs in the case when the layer surface is horizontal, $0^m(x, t)$ lies in the midpoint of the slabs. One can observe the field leakage at the core edges, which can be described by the scattering function as

$$B_z^i(x, y, t) = B_z^*(x, y, t)f_d(x, y, t). \quad (15)$$

Parameters for this function, defined on assumption that the magnetic currents in the regions between the slabs (S^{in}) and those outside (S^{out}) are equal, can be obtained by minimizing the functional

$$\left| \int_{S^{\text{out}}} B_z^i(x, y, t) dx dy - \int_{S^{\text{in}}} B_z^i(x, y, t) dx dy \right| \rightarrow 0. \quad (16)$$

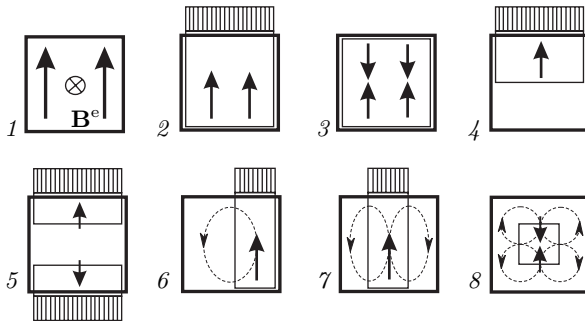
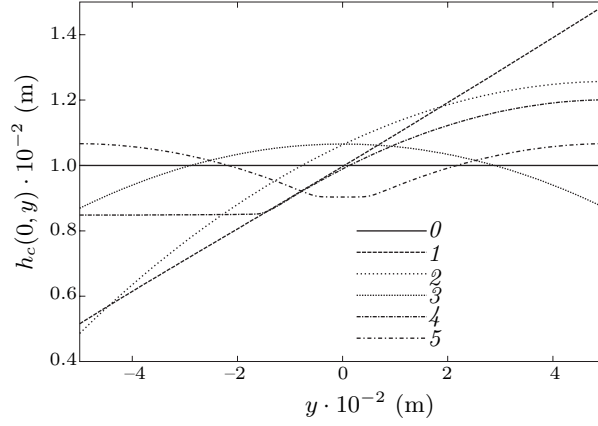


Fig. 2. Location of core generating electromagnetic forces: potential forces $\omega_F = 0$ (types 1–5) and forces with a vortex component $\omega_F \neq 0$ (types 6–8).

Fig. 3. Profiles for the equilibrium position of the layer free surface under potential electromagnetic forces ($\omega_F = 0$): numbers 1–5 correspond to the notation from Fig. 2 ($S\beta\gamma = 1.63 \cdot 10^6$, $G = 10^8$, $B^e = 0.2$ Tl for type 1), θ – the horizontal position of the layer.



Being subjected to the electromagnetic force $F_y(x, y, t) = j_x(x, t)B_z(x, y, t)$, the layer surface can reach the equilibrium position $h_c(x, y)$, different from the horizontal one. We examine two types of the equilibrium state, one of which involves the value

$$\omega_F = \int_{-a}^a \int_{-b}^b |\nabla \times \mathbf{F}| dx dy \quad (17)$$

equal to zero, and the other – different from zero. Schemes of variants capable of providing $\omega_F = 0$ and $\omega_F \neq 0$ are represented in Fig. 2, where bold arrows denote electromagnetic forces, and the dashed line indicates the flows of the liquid. Fig. 3 presents the cross-sections of the surface in equilibrium position $h_c(0, y)$ for $\omega_F = 0$. Fig. 4 shows the surface at equilibrium position and the velocity field for $\omega_F \neq 0$. The equilibrium position of the surface is reached by the balance between hydrostatic, electromagnetic and centrifugal forces.

4. Stability of the layer free surface. Conclusions. We have studied the stability $h_c(x, y)$ in the analysis of the mathematical model formalized in equations (4)-(8) and (13)-(16) by numerical calculations. Deviations of the free surface from equilibrium position $\zeta = h(x, y, t) - h_c(x, y)$ at the origin of the process time are represented as a long small-amplitude wave. One of the observed

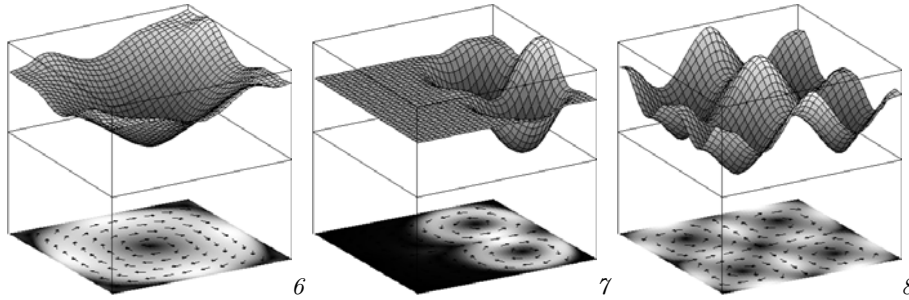


Fig. 4. Free surfaces and velocity fields for the equilibrium position under electromagnetic forces with a vortex components $\omega_F \neq 0$: numbers 6–8 correspond to the notation from Fig. 2 ($S\beta\gamma = 2.61 \cdot 10^5$, $G = 10^8$).

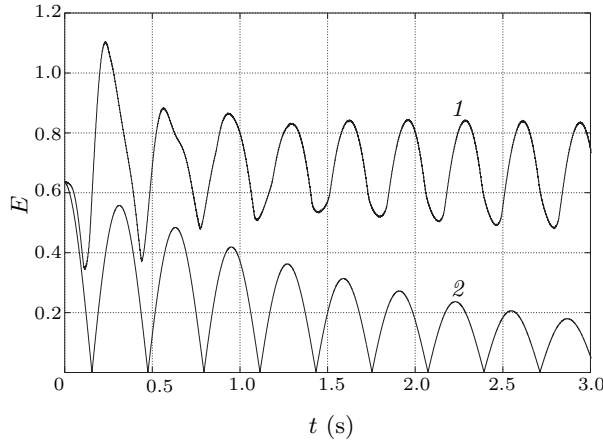


Fig. 5. Evolution of the functions E in a non-decaying oscillation process (1) for type 3 in Fig. 2 ($S\beta\gamma = 6.52 \cdot 10^6$, $G = 10^8$) and in the process of gravity waves decaying (2).

parameters is the integral value $|\zeta|$ for the whole layer:

$$E(t) = \int_{-b}^b \int_{-a}^a |\zeta(x, y, t)| dx dy. \quad (18)$$

For the cases with $\omega_F = 0$, the instability mechanism can be explained as follows. The probability of the long-wave disturbances of the surface with the wave vector directed along the current density vector changes the value of current density along this direction. It disturbs the balance between electromagnetic and gravity forces at equilibrium state and can stop disturbance decaying under certain parameters of the process. In the case of acting by an uniform external magnetic field (type 1 in Fig. 2) two mechanisms of influence on the disturbances can be implemented. In an unstable process the disturbances grow under electromagnetic forces near one edge, where h_c is minimal and are suppressed near the opposite edge, where h_c is maximal. Location type 2 of cores (Fig. 2) with a nonuniform magnetic field (and forces) is characterized by a lower stability if compared to type 1 (when $B^e = B_0$), which is attributed to the absence of an additional mechanism of oscillation suppression. Of the proposed types, type 3 is the most unstable because of the presence of the mechanism of disturbance growth on the both sides of the layer. The function E for an unstable processes does not decay (Fig. 5). As to types 4 and 5, we can say that these are stable against disturbances, which are attributed to the presence of the mechanism of disturbances suppression on the one or both sides of the layer and the absence of a mechanism of disturbance

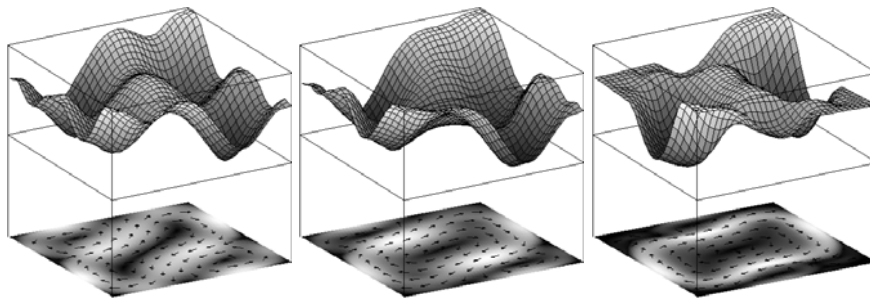
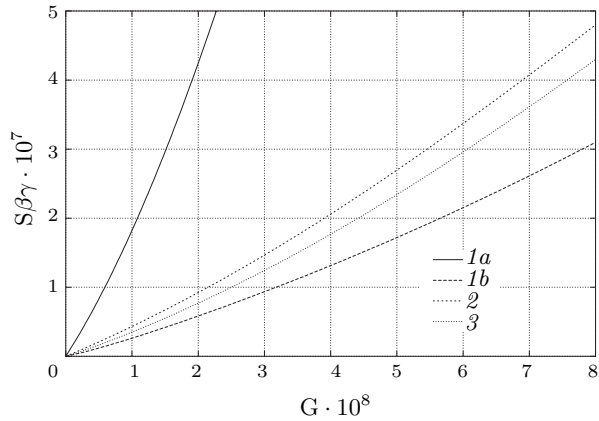


Fig. 6. Snapshots of the free surfaces and the velocity fields in an unstable process for type 8 in Fig. 2 ($S\beta\gamma = 1.63 \cdot 10^6$, $G = 10^8$).

Fig. 7. Neutral curves for the processes with $\omega_F = 0$: *1a* – for type 1 (Fig. 2) with $B^e = 0.015$ Tl, *1b* – for type 1 with $B^e = 0.2$ Tl, *2* and *3* – for types 2 and 3.

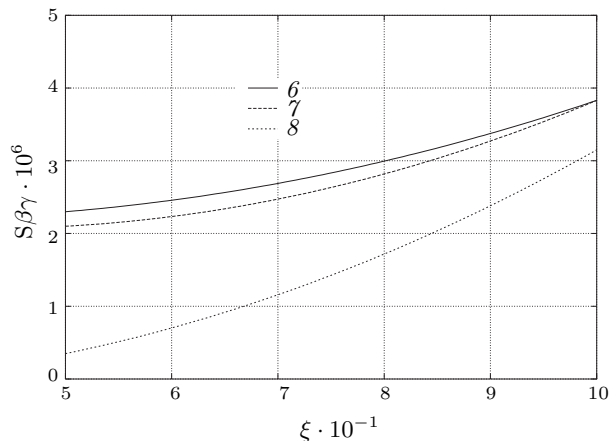


growth. Fig. 7 presents neutral curves for all described cases except types 4 and 5. For type 1 an increase in value of the external magnetic field B^e decreases the stability threshold.

For the cases with $\omega_F \neq 0$, there is an additional, just discussed, instability mechanism, related to a nonlinear interaction between the vortex motion and the oscillation process. The process with a more intensive four-eddies liquid flow (type 8, Fig. 2) is less stable than one- and two-eddies flows (types 6, 7) due to a higher degree of the nonlinear interaction. When the process is stable, the velocity field with four eddies, for example, and equilibrium position of the surface are stationary for a long time. If the process is unstable, the eddies placed in diagonal change their intensity periodically. After that one large eddy is shaped and long wave surface oscillations appear (Fig. 6), as it was noticed in experiment [9]. Fig. 8 gives neutral curves for types 6–8 of electromagnetic forces generation. The increase in slabs size (increase in ξ) improves the stability of the system due to a decrease in the scale of the vortex motion. In the limiting case, when the slabs cover the layer plane completely ($\xi = 1$), the initial vortex flow is absolutely suppressed.

The obtained results allow to conclude that the free surface of the plane layer of a conducting liquid subjected to electromagnetic forces could be unstable against disturbances. This fact should be taken into account in designing technological MHD-devices.

Fig. 8. Neutral curves for the processes with $\omega_F \neq 0$. Numbers correspond to the notation from Fig. 2 ($G = 10^8$).



5. Acknowledgements. The research described in this publication was made possible in part by Award No. YSF 2002-424 from the International Association for the promotion of co-operation with scientists from the New Independent States of the former Soviet Union (INTAS) and by Award No. PE-009-0 of the U.S. Civilian Research & Development Foundation for the Independent States of the Former Soviet Union (CRDF).

REFERENCES

1. A. SHISHKO. Wave processes at the surface of a magnetohydrodynamically buoyed fluid. *Magnetohydrodynamics*, vol. 28 (1992), no. 2, pp. 170–181.
2. I. KOLESNICHENKO, S. KHRIPCHENKO. MHD-instability of the equilibrium state of the surface of a conductive liquid thin layer. *Magnetohydrodynamics*, vol. 37 (2001), no. 4, pp. 360–365.
3. V. KOLESNICHENKO, S. KHRIPCHENKO. Surface oscillations in the liquid cathode aluminium of an electrolytic cell. *Magnetohydrodynamics*, vol. 25 (1989), no. 3, pp. 392–395.
4. S. KHRIPCHENKO. Electro-vortex flows in thin conductive liquid layers. *Magnetohydrodynamics*, vol. 27 (1991), no. 1, pp. 115–118.
5. V. ZYMIN, S. KHRIPCHENKO. Two-dimensional representation of the magnetohydrodynamic equations of flow in plane-parallel channels with ferromagnetic cores. *Magnetohydrodynamics*, vol. 15 (1979), no. 4, pp. 461–465.
6. V. BARANNIKOV, V. ZYMIN. Instability of the rest of isothermal conducting liquid placed in the gap between ferromagnetic blocks with flowing of electrical current. *Magnetohydrodynamics*, vol. 18 (1982), no. 3, p. 141.
7. V. ALMUKHAMETOV, S. KHRIPCHENKO. Electro-vortex flow mechanisms for an electrolyzer containing a solid anode. *Magnetohydrodynamics*, vol. 23 (1987), no. 3, pp. 317–319.
8. S. KHRIPCHENKO, M. MANN. Semiempirical model of the hydrodynamic processes in the bath of an aluminium electrolyzer. *Magnetohydrodynamics*, vol. 28 (1992), no. 1, pp. 77–84.
9. V. ALMUKHAMETOV, S. KHRIPCHENKO. Physical modelling of unstable state of electrolyte – liquid metal interface in high-power aluminum cells. *Dokl. Akad. Nauk SSSR*, vol. 302 (1988), no. 4, pp. 845–847 (*in Russ*).
10. S. DENISOV, V. DOLGIH, S. KHRIPCHENKO. Electro-vortex Flow in Flat Channel. *Thes. MTLM Int. Workshop*, (1999), pp. 291–295.
11. V. KOLESNICHENKO, A. PICHUGIN, S. KHRIPCHENKO. Numerical studies of plane electro-vortex flows in a two-layer conducting fluid. *Magnetohydrodynamics*, vol. 25 (1989), no. 3, pp. 332–336.
12. V. ALMUKHAMETOV, V. KOLESNICHENKO, S. KHRIPCHENKO. Mathematical model of plane electrical eddy flows in a two-layer conducting fluid. *Magnetohydrodynamics*, vol. 24 (1988), no. 2, pp. 260–263.

Received 3.04.2003